Nanoencapsulation of a glucocorticoid improves barrier function and anti-inflammatory effect on monolayers of pulmonary epithelial cell lines

Lucas A. Rigo [a], Cristiane S. Carvalho-Wodarz [b], Adriana R. Pohlmann [c], Silvia S. Guterres [a], Nicole Schneider-Daum[b], Claus-Michael Lehr [b], Ruy C.R. Beck [a]

[a]*Programa de Pós-Graduação em Ciências Farmacêuticas, Faculdade de Farmácia, Universidade Federal do Rio Grande do Sul, Av. Ipiranga, 2752, 90610-000, Porto Alegre, RS, Brazil*

[b]*Drug Delivery (DDEL), Helmholtz-Institute for Pharmaceutical Research Saarland (HIPS), University Campus, Building E8.1, D-66123 Saarbrücken, Germany*

[c]*Departamento de Química Orgânica, Instituto de Química, UFRGS, Av. Bento Gonçalves 9500, 91501-970, Brazil*

* Corresponding author:

Ruy C. R. Beck (ruy.beck@ufrgs.br)

Faculdade de Farmácia - UFRGS

Av. Ipiranga, 2752, 4º andar 90610-000 Porto Alegre-RS Brazil

Phone: +55 051 3308 5951 Fax: +55 051 3308 5243

Abstract

The anti-inflammatory effect of polymeric deflazacort nanocapsules (NC-DFZ) was investigated, and possible improvement of epithelial barrier function using filter grown monolayers of A549 and Calu-3 using as models was assessed. NC prepared from poly(ε-caprolactone) (PCL) had a mean size around 200 nm, slightly negative zeta potential (~ - 8 mV), and low polydispersity index (< 0.10). Encapsulation of DFZ had an efficiency of 85% and loading rate of 0.5 mg/ml. No cytotoxic effects were observed at particle concentration of 9.85 x 10^{11} NC/ml, which was therefore chosen to evaluate the effect of NC-DFZ at 1% (w/v) of PCL and 0.5% (w/v) of DFZ on the epithelial barrier function of Calu-3 monolayers. Nanoencapsulated drug at 0.5% (w/v) increased transepithelial electrical resistance and increased permeability of the paracellular marker sodium fluorescein, while non-encapsulated DFZ failed to improve these parameters. Moreover, NC-DFZ reduced the lipopolysaccharide (LPS) mediated secretion of the inflammatory marker IL-8. *In vitro* dissolution testing revealed controlled release of DFZ from nanocapsules, which may explain the improved effect of DFZ on the cells. These data suggest that nanoencapsulation of pulmonary delivered corticosteroids could be advantageous for the treatment of inflammatory conditions, such as asthma and chronic obstructive pulmonary diseases.

Keywords: A549 cells, Calu-3 cells**,** deflazacort, glucocorticoid, polymeric nanocapsules, pulmonary delivery.

1. Introduction

As advanced drug carriers systems, nanocapsules (NC) have relevant technological advantages in the pharmaceutical field, such as the ability not only to avoid the burst release of drugs, but also to improve the effects of bioactive compounds [1-4]. The promising results reported for poly(ε-caprolactone)-based nanoparticles make such NC interesting from the pharmaceutical technology standpoint, due to the broad applications in various therapeutic targets, like cutaneous [5] and parenteral delivery [6, 7].

Lungs represent an attractive route for the administration of inhalation nanopharmaceuticals, as this class of drugs affords to control release and thus premature pulmonary clearance of locally topically acting drugs. [8-10]. This is particularly true for anti-inflammatory drugs used to control diseases such as asthma and chronic obstructive pulmonary disease (COPD). In most cases glucocorticoids are the first choice therapy due to their anti-inflammatory activity, which is based mainly on the downregulation of proinflammatory cytokines [11, 12].

Human cell culture models have attracted increasing interest as a preclinical tool to assess toxicity and efficacy of active pharmacological ingredients and their formulations [13], also affording to reduce the use of animals [13, 14]. Previous studies have demonstrated that the physicochemical characteristics of NC such as surface charge [15], stabilizers and polymers [16, 17] may trigger cytotoxic effects, which could limit their applications. Therefore, studies of the interaction between nanoparticles and biological systems are needed in order to improve current understanding of the phenomenon and to design innovative nanocarriers for therapeutic applications.

This study evaluated the safety and efficacy of poly(ε-caprolactone)-based NC as potential nanocarrier for pulmonary delivery. For this purpose, cytotoxicity studies of these NC were carried out in representative human alveolar (A549) and bronchial (Calu-3) epithelial cell models. The maximally tolerated dose using the number of particles was determined as a parameter of cytotoxicity. Furthermore, the effect of the nanoencapsulation of the glucocorticoid deflazacort (DFZ) on the epithelial barrier function as measured by transepithelial electrical resistance (TEER) has been assessed. Similarly, the ability to reduce the expression of IL-8 in Calu-3 was also evaluated. DFZ was chosen due to its higher anti-inflammatory activity and lesser side effects, compared with other corticosteroids [18].

2. Material and methods

2.1. Materials

Poly(ε-caprolactone) (PCL) (MW: 80.000) was purchased from Sigma-Aldrich (São Paulo, Brazil) and medium-chain triglycerides (MCT) were bought from Delaware (São Paulo, Brazil). Polysorbate 80 was supplied by Henrifarma (São Paulo, Brazil) and deflazacort was purchased from Pharma Nostra (São Paulo, Brazil). Lipopolysaccharide (LPS) from *Escherichia coli* O111.B4 was purchased from Sigma® (St. Louis, USA). Sigma Dialysis bags (Spectra Por 7, 10 kD, Spectrum Laboratories, USA) were purchased from Bioagency (São Paulo, Brazil). HPLC grade acetonitrile was acquired from Tedia (São Paulo, Brazil). An analytical balance was used do weigh all the solid chemicals (Model AUX 220, Shimazdu Corporation, Kyoto, Japan). All other chemicals and solvents used in this study were of pharmaceutical grade and were used as received.

2.2. Preparation of polymeric nanocapsules

NC suspensions were prepared by interfacial deposition of preformed polymer [19, 20]. Two solutions were prepared (organic and non-organic phases). The organic phase consisted of an acetone solution (67 ml) containing poly(ε-caprolactone) (0.25 g) and MCT (0.75 ml) as oily core. The formulations containing glucocorticoid were prepared adding DFZ to this phase in order to obtain a loading rate of 0.5 mg/ml, and were called NC-DFZ. The aqueous phase (134 ml) contained a surfactant with a high hydrophilic-lipophilic balance (HLB) value (polysorbate 80) (0.193 g). The organic phase was slowly injected under moderate magnetic stirring into the aqueous phase. After, acetone was removed and the NC suspension concentrated by evaporation (bath at 40 °C) under reduced pressure using a rotavapor (Rotavapor RII, Büchi, Flawil, Switzerland). The final formulation was adjusted to 25 ml. All formulations were prepared in triplicate, stored at room temperature (25 ± 2 °C) and protected from light in amber glass flasks upon analysis.

2.3. Characterization of the polymeric nanocapsules

2.3.1. Particle size, polydispersity index and zeta potential

The granulometric profile was determined by light diffractometry (Mastersizer, Malvern Instruments, Worcestershire, UK) as volume-weighted ($d_{v,4.3}$). Span values were calculated using Eq. (1):

$$\text{Span} = (d_{0.9} - d_{0.1})/ d_{0.5} \qquad (1)$$

where $d_{0.9}$, $d_{0.5}$ and $d_{0.1}$ are the particle diameters determined respectively at the 90th, 50th, and 10th percentile of undersize particles. The Span value reflects the range of the size distribution. Smaller Span values represent narrower size distributions.

Particle size and polydispersity index (PDI) were determined by photon correlation spectroscopy (three measurements/batch; two runs of 30 s/measurement, 25 °C) after adequate dilution of an aliquot of the suspensions in purified water (Zetasizer Nanoseries, Malvern Instruments, Worcestershire, UK). Zeta potentials were determined using the same instrument at 25 °C, after the dilution of the samples in 10 mM NaCl in aqueous solution (three measurements/batch; 10 runs/measurement, 25 °C).

2.3.2. Determination of loading rate and encapsulation efficiency

Loading rate was determined after dissolution of an aliquot (200 µl) of nanocapsules suspension in 10 ml of mobile phase followed by ultrasound for 10 min and quantified by liquid chromatography (LC) using a previously validated methodology [21]. The chromatographic system consisted of a Gemini RP-18 column (250 mm x 4.6 mm, 5 µm, Phenomenex Torrance, USA) and Shimadzu instrument (LC-10AVP Pump, UV-vis SDP-10AVP, Japan). The mobile phase (at a flow rate of 1.0 ml/min) was composed of acetonitrile/water (80:20%, v/v), the volume of injection was 20 µl, and DFZ was detected at 244 nm. The method was linear (r^2 = 0.9999) in the range of 5-40 µg/ml, accurate (recovery: 95.75 ± 0.5 %), and precise (R.S.D.: < 1.41% for repeatability and < 2.37 for intermediate precision). Specificity was tested in the presence of the suspension adjuvants, when these factors were shown not to alter the DFZ assay.

The encapsulation efficiency (%) was determined by the difference between total drug (loading rate) and free DFZ concentration. Free DFZ (non-associated to nanostructures) was determined in the ultrafiltrate after separation of the nanoparticles by ultrafiltration/centrifugation (Ultrafree-MC10.000 MW, Millipore, UDA), at 1000 rcf for 10 min. All analysis were performed in triplicate.

2.4. Particle concentration and surface area

The nanocapsule number density (NC/ml) of suspension was determined using two independent methods: turbidimetry and nanoparticle tracking analysis (NTA).

2.4.1. Turbidimetry

Turbidy τ (cm^{-1}) was determined according to a previously described method [22, 23]. Firstly, the lower wavelength in the UV-visible region, where there is no photon absorption, was determined in order to guarantee that scattering was the only phenomenon of the interaction between light and matter due to the presence of the particles in suspension. The wavelength of 382 nm was chosen based on a sample of NC suspension analyzed using a Shimadzu® UV-160PC spectrophotometer. Then, three batches of nanocapsules suspension were prepared and diluted (MilliQ® water) in such a range so as to obey the Lambert-Beer law. Turbidy (τ) was calculated from the absorbance signal A of the equipment, as given in Eq. (2):

$$\tau = \frac{1}{b}\ln(10) \cdot A \qquad (2)$$

where b (cm) is the optical cell path length, τ is a function of the particle diameter d (cm), N is the particle concentration N (particles cm^{-3}), Q is a dimensionless quantity, which is the extinction efficiency as following Eq. (3):

$$\tau = \frac{\pi}{4} d^2 \cdot N \cdot Q (3)$$

At a fixed relative refractive index, it is possible to calculate Q as given in Eq. (4):

$$Q = \frac{K \cdot 2\ln(10) \cdot \alpha \cdot d}{3} \qquad (4)$$

where d (cm) is the particle diameter, α (g cm^{-3}) is the particle density, and K (cm^2 g^{-1}) is the sample extinction coefficient, calculated using the Eq. (5):

$$\tau = \ln(10) \cdot K \cdot c \qquad (5)$$

where c (g cm^{-3}) is the sample concentration.

2.4.2. NTA analysis

NTA analysis was performed using a NanoSight® LM10 (NanoSight, Amesbury, UK), equipped with a sample chamber with a 640-nm laser. This technique is based on particle-tracking software able to measure the light scattered from nanoparticles in suspension. So, the NC suspensions were diluted (20.000x) in MilliQ® water and injected in the pre-calibrated chamber with a syringe. The light scattered was tracked by a digital camera for 60 s. The software identifies the frame-to-frame motions of each individual nanoparticle through Brownian motion and relates the movement to particle size. It provides the nanoparticle concentration and the hydrodynamic-size distribution [24, 25].

2.4.3. Surface area (S)

The surface area (cm²/ml) of the nanocapsules was calculated from the result of the number of particles according to a previous study [26] using Eq. (6):

$$S = 4\pi \left(\frac{d}{2}\right)^2 . N(6)$$

where d (cm) is the particle diameter and N represents the number of nanocapsules per ml of suspension.

2.5. Cell cultures

The A549 cells (CCL-185; ATCC, Manassas, VA, USA) and Calu-3 (HTB-55; ATCC, Manassas, VA, USA) cell lines were grown using 75 cm² (T-75) flasks in humidified 5% CO_2/95% atmospheric air incubator at 37°C. For A549 cells, RPMI-1640 with L-glutamine (PAA Laboratories GmbH, Pasching, Austria) supplemented with 10% fetal calf serum (FCS) (Lonza, Biosciences) was used as cell culture media (CCM). For Calu-3 cells, the cell culture media used was Minimum Essential Medium (MEM) with Earl's Salts and L-glutamine (PAA Laboratories GmbH, Pasching, Austria) and supplemented with 10% FCS, 1% non-essential amino acid (NEAA) solution and 1 mM sodium pyruvate (all from Sigma–Aldrich GmbH, Germany).

2.6. Cytotoxicity assays

Confluent A549 or Calu-3 cells were washed with buffered phosphate saline (PBS) and detached using trypsin-EDTA solution. Then, cells were pelleted by centrifugation for 4 min at 300 rcf. Supernatant was removed and the cell pellet formed was suspended in cell culture media. The number of cells was counted using an automated cell counter (CASY, Roche Innovatis AG, Germany). A549 (10,000 cell/well) or Calu-3 (50,000 cell/well) were seeded separately into 96-well plates and incubated until cells reached confluence. After, cell culture media containing NC of three different particle concentrations (9.85 x 10^{10}, 9.85 x 10^{11}, and 4.92 x 10^{12} NC/ml of cell culture media) were incubated in the cells for 2, 24, and 48 h. The respective

surface areas calculated from these particle concentrations were 1.24 x 10^2, 1.24 x 10^3, and 6.18 x 10^3 cm^2/ml.

In order to evaluate whether the surfactant of the NC (polysorbate 80) has any influence on NC cytotoxicity, an aqueous phase was prepared containing polysorbate 80 at the same concentration as used in the suspensions. Then, aliquots containing 0.03, 0.33, and, 1.60 mg/ml of polysorbate 80, whose volumes corresponded to 9.85 x 10^{10}, 9.85 x 10^{11}, and 4.92 x 10^{12} NC/ml respectively, were also prepared and evaluated in the cytotoxicity assays under the same cell culture media conditions as used for the NC suspension. The supernatant from cell cultures was collected to assess lactate dehydrogenase (LDH) release, while the adherent cells were lysed to assess metabolic activity with Alamar blue (AB), as described below. All experiments were performed in triplicate.

2.6.1. Lactate dehydrogenase assay (LDH):

The LDH assay (Cytotoxicity Detection Kit, Roche Diagnostics GmbH, Germany) is based on the measurement of lactate dehydrogenase released from the cytosol of dead or plasma membrane-damaged cell assayed in cell culture media. At each predetermined time, supernatants (100 µl) were transferred to 96-well plates and an equal volume of the LDH reagent mixture was added to each well. Absorbance was measured at 492 nm, cytotoxicity (%) was calculated using Triton X-100 as positive control (100% cytotoxicity), while cells with cell culture media were used as negative control (0% cytotoxicity), according to Eq. (7):

$$\%\ cytotoxicity = Abs_{exp}^{492} - Abs_{low\ control}^{492} / Abs_{high\ control}^{492} - Abs_{low\ control}^{492}\ x\ 100 \qquad (7)$$

2.6.2. Alamar Blue (AB) assay:

Cell viability was evaluated using the AB assay (Life Technologies, Carlsbad, CA, USA). AB measures cell proliferation from the indicator resazurin (oxidized form). This indicator is blue and non-fluorescent; however, resorufin (reduced form) is red and highly fluorescent. Thus, alterations in the cellular metabolic activity mediated by mitochondrial enzymes can be detected [27, 28]. The reduction of AB is mediated by mitochondrial enzymes. In this assay, cells were washed with PBS and a solution containing 5% (v/v) of AB reagent prepared in fresh cell culture media was added to each well. After 3 h of incubation, AB fluorescence was measured at 540 and 595 nm of excitation and emission wavelengths, respectively. The positive and negative controls used in this experiment were prepared as described for the LDH assay. The results of both LDH and AB were quantified using a plate reader (Infinite M200 PRO, TECON, Austria).

2.7. Influence of NC on the epithelial barrier of Calu-3 cells

2.7.1. Transepithelial electrical resistance (TEER)

Calu-3 cells were seeded (100.000 cells/ml) in multiwell plates (Costar Transwell® 3460, 12 well, pore size 0.4 µm, Corning, USA) and cultivated under liquid covered condition (LCC), in which cell culture media was added in both apical (0.5 ml) and basolateral compartments (1.5 ml). TEER values were determined before and after NC incubation using a voltmeter (STX-2 EVOM®, World Precision Instruments, UK). Nanocapsules (9.85 x 10^{11} NC/ml) without (NC) or with DFZ (NC-DFZ) as well as free drug (Free-DFZ) were incubated on confluent cells for 2, 24, and 48 h at 37°C. TEER values were calculated by subtracting the resistance of the membrane without cells (120 Ω) and the result corrected based on the area of inserts (1.12 cm^2).

2.7.2 Cell permeability to sodium fluorescein (FluNa)

Calu-3 cell monolayers were used for the permeability studies after 7-8 days of seeding, following a previous protocol [29]. After 24 h of the incubation of NC (9.85 x 10^{11} NC/ml) or NC-DFZ (at 0.5%), cell culture media of both apical and basolateral compartments were aspired and incubated with Krebs-Ringer buffer (KRB) for 30 min at 37°C until equilibrium was reached. Sodium fluorescein permeability was evaluated by replacing KRB in the basolateral compartment and adding 20 µl of fluorescein solution (10 µg/ml) to KRB in the apical chamber (donor). Immediately, 20 µl of the solution in the apical side was withdrawn to determine initial concentration. Cells were incubated at 37°C and 200-µl aliquots were retrieved from the basolateral chamber (acceptor) after 0.5, 1, 1.5, 2, 2.0, and 3 h. The sample volume (200 µl) removed was replaced with fresh pre-warmed KRB. During the test, the samples were transferred to 96-well plates, and fluorescence was measured using a fluorimeter (Infinite M200 PRO, TECON, Austria). The excitation and emission wavelengths were 488 and 530 nm, respectively. Apparent permeability coefficients (P_{app}) were calculated using Eq. (8):

$$P_{\text{app}}\,(cm/s) = (dq/dt) \cdot \left(1/AC_0\right) \qquad (8)$$

where dq/dt represents the linear transport rate of sodium fluorescein, A is the surface area of the insert, and C_0 is the initial concentration of sodium fluorescein in the apical chamber. For comparison, the permeability of sodium fluorescein for the non-encapsulated form of DFZ (Free-DFZ) was also performed.

2.8. Interleukin-8 (IL-8) measurement

Interleukins are involved in several inflammatory diseases [11]. IL-8 is the main chemotactic mediator released by pulmonary epithelial cells [30], while LPS (a bacterial endotoxin) promotes the secretion of this cytokine [31]. Thus, the influence of the nanoencapsulation of DFZ on the expression of IL-8 was evaluated. Confluent Calu-3 cells were stimulated with LPS (+LPS) at 100 ng/ml 24 h before exposure to NC, NC-DFZ (at 0.5%), or Free-DFZ (0.5%). The particle concentration used for NC and NC-DFZ was 9.85 x 10^{11} NC/ml. Non-encapsulated form of DFZ at 0.5% (Free-DFZ) was used. For comparison, experiments without LPS (-LPS) were carried out. After 24 and 48 h of exposure, aliquots of supernatants were collected and stored at -80°C upon analysis. IL-8 release was detected by flow cytometry using a FACScalibur flow cytometer (BD Biosciences®) and a cytometric beads array kit (CBA). The results were analyzed using the FACP Array™ software.

2.9. In vitro drug release

In vitro DFZ release profile of NC-DFZ was evaluated (*n=3*) using the dialysis bag method [19, 20] and polysorbate 80 at 2 % (w/v) in water as medium at 37 °C. This concentration was previously tested in order to maintain sink conditions. The dialysis bag containing 1 ml of the sample (0.5 mg/ml) was placed in a 250-ml flask containing 200 ml of release medium under constant moderate stirring. The amount of 1 ml of the external medium was withdrawn from the system at a predetermined time interval, replaced by an equal volume of fresh medium, and filtered through a 0.45-µm membrane. DFZ was assayed in the samples by liquid chromatography (LC) according to the methodology previously described, as mentioned in section *2.3.2* [21]. The diffusion of non-encapsulated form of DFZ across the dialysis bag was performed and

used as control. For this purpose, an ethanol solution of DFZ (DFZ-ES) at the same NC concentration was prepared.

2.10. Statistical analysis

Statistical analysis was carried out by analysis of variance (ANOVA). Post-hoc multiple comparisons were carried out applying Tukey's test at p-value ≤ 0.05 (SigmaStat® Statistical Program, Version 3.5, Jandel Scientific, USA).

3. Results

NC suspensions had a unimodal particle size distribution in the nanoscale range, as analyzed by laser diffractometry (Fig. 1).

In addition, the particle size distribution profile obtained by laser diffraction showed a narrow range, with Span values lower than 1.7 (Table 1).

The measurements performed by photon correlation spectroscopy revealed that NC had mean particle size around 200 nm, polydispersity indexes below 0.1, pH value around 6.0, and zeta potential close to neutral (Table 2). Moreover, the NC formulation containing the DFZ (NC-DFZ) had loading rate of 4.9 ± 0.03% and encapsulation efficiency of 85 ± 0.06%.

The particle concentration of NC obtained using the spectroscopic method was $1.73 \pm 0.46 \times 10^{13}$ nanocapsules per ml of suspension. On the other hand, particle concentration obtained using the NTA method was $N = 2.29 \pm 0.45 \times 10^{13}$ nanocapsules per ml of suspension ($p > 0.05$).

Fig. 2 shows the results obtained using the LDH method after the incubation of NC in three different particle concentrations (9.85×10^{10}, 9.85×10^{11} or 4.92×10^{12}

NC/ml) for 2, 24, and 48 h in A549 or Calu-3 cells. The particle concentration 4.92 x 10^{12} NC/ml was cytotoxic to A549 (Fig. 2A) and Calu-3 cells (Fig. 2B). On the other hand, no cytotoxic effect was observed for 9.85 x 10^{10} and 9.85 x 10^{11} NC/ml particle concentrations in both A549 and Calu-3 cells.

Fig. 3 shows the cell viability using the AB method in A549 (Fig. 3A) and Calu-3 (Fig. 3B) cells exposed to three different particle concentrations (9.85 x 10^{10}, 9.85 x 10^{11} or 4.92 x 10^{12} NC/ml) for 2, 24, and 48 h. Both pulmonary cells remained metabolically active after 48 h of exposure to 9.85 x 10^{10} and 9.85 x 10^{11} NC/ml. However, the nanoparticle solution containing 4.92 x 10^{12} NC/ml was harmful to the cells after 48 h of exposure, in comparison with the concentrations of 9.85 x 10^{10} and 9.85 x 10^{11} NC/ml.

Fig. 4 shows the results obtained in the LDH method for both A549 (Fig. 4A) and Calu-3 (Fig. 4B) cells exposed only to polysorbate 80 (surfactant), which was used to prepare the NC suspensions.

In this test, three different concentrations of surfactant (0.03, 0.33, and 1.60 mg/ml), which correspond to its amount in 9.85 x 10^{10}, 9.85 x 10^{11} or 4.92 x 10^{12} NC/ml were evaluated. As can be observed, polysorbate 80 did not show any cytotoxic effects in A549 neither Calu-3 cells at any of the concentrations tested. In the same way, Fig 5 shows the cell viability test using the AB method for the same concentrations of surfactant described above. Both A549 (Fig. 5A) and Calu-3 cells (Fig. 5B) remained metabolically active, with survival rate ranging from 80 to 100% for 48 h.

Fig. 6 shows the TEER measurements of the Calu-3 cells 24 h before and 2, 24, and 48 h after exposure to the treatments with NC and NC-DFZ (at 9.85 x 10^{11} particles NC/ml) and non-encapsulated DFZ (Free-DFZ). Within 24 h, the TEER of NC-DFZ

treated cell cultures was significantly increased ($p < 0.05$) compared to all other treatments. After 48 h such difference was no longer observed.

Fig. 7 shows the results obtained from the transport of sodium fluorescein across Calu-3 cell layers after 24 h of incubation with NC, NC-DFZ, and non-encapsulated DFZ. The P_{app} results revealed the following values: $1.63 \pm 0.19 \times 10^{-6}$ cm/s), $1.87 \pm 0.16 \times 10^{-6}$ cm/s, and $1.87 \pm 0.20 \times 10^{-6}$ cm/s for NC-DFZ, NC and non-encapsulated DFZ, respectively. All results were significantly lower than the value obtained in cultures containing only the cell culture media ($2.34 \pm 0.05 \times 10^{-6}$ cm/s).

Fig. 8A and Fig. 8B show the levels of IL-8 cytokine in Calu-3 cells stimulated or not with LPS, respectively, after 24 and 48 h. Interleukin was quantified after the incubation of NC, NC-DFZ, and non-encapsulated DFZ (Free-DFZ). Regarding the non-stimulated LPS (Fig. 8A), IL-8 results for the control (cell culture media) and NC did not differ significantly, regardless of exposure time ($p > 0.05$). No significant differences were observed between the treatments containing the anti-inflammatory drug (NC-DFZ and Free-DFZ) and the control, after 24 h ($p > 0.05$). The results obtained for both NC-DFZ and Free-DFZ showed significant differences in comparison with the control ($p \leq 0.05$) after 48 h, but not after 24 h. On the other hand, regarding the results obtained for stimulation with LPS (Fig. 8B) the non-encapsulated form of DFZ (Free-DFZ) showed a decrease in IL-8 expression in comparison with the control ($p \leq 0.05$) after 24 h as well as after 48 h. In other words, the nanoencapsulated form of DFZ (NC-DFZ), caused no difference in IL-8 release after 24 h, compared to the control (CMM). However, this effect was observed only after 48 h ($p > 0.05$) (Fig. 8B).

The results obtained from *in vitro* drug release profiles of non-encapsulated DFZ in an ethanolic solution (DFZ-ES) and from NC (NC-DFZ) are depicted in Fig 9.

As can be observed, DFZ showed a faster diffusion through the dialysis bag from DFZ-ES. The amount of drug diffused after 8 h was around 90%, whereas DFZ released from NC reached only 35% in the same period. The amount of DFZ released from nanocapsules was about 50% and 83% after 24 and 48 h, respectively.

4. Discussion

As drug delivery systems, polymeric nanocapsules offer interesting technological advantages, especially concerning the ability to control drug release, in order to improve therapeutic efficacy. The nanometric size of these suspensions is one of the main factors behind these advantages, and makes them an interesting target for research and design of innovative products [2, 5, 19, 32, 33]. In this work, the safety of NC prepared with poly(ε-caprolactone) as potential pulmonary drug delivery nanocarrier was studied using the glucocorticoid DFZ as drug. Furthermore, the influence of the nanoencapsulation of the DFZ on the epithelial barrier function and inflammatory response in pulmonary cells models was evaluated.

Regarding the size of NC, all formulations showed the same size range (around 200 nm), independently of the presence of the drug. These results are consistent with other data reported in the literature for NC prepared by interfacial deposition of pre-formed polymer using PCL and non-ionic surfactants [1, 20, 34]. NC had a slight negative zeta potential, explained by the non-ionic coating layer (polysorbate 80) at the particle/water interface, which sterically stabilizes these nanoparticles [35]. Since any particle acquires charge in suspension, these NC could be considered neutral. This result is in agreement with similar NC suspensions prepared using PCL as polymer and polysorbate 80 as stabilizer that showed zeta potential values of up to -8 mV and physical stability for at least 9 months [19, 33]. Also, the NC prepared with DFZ

showed a loading rate of about 5 % (w/w), with 85 % (w/v) of drug loaded on the nanocapsules and 15% (w/v) as non-encapsulated drug (dispersed in water).

The total mass of a drug is classically used in pharmacology as a parameter of dose. In NC suspensions, where the solid and liquid states coexist, the high surface area of the particles induces interactions with biological systems and, for this reason, drugs or other active compounds may be delivered. Therefore, total mass is not predictive of surface area. However, the surface area may be evaluated calculating the number of particles in suspension. The estimation of the particle concentration is complex. This task involves a variety of methods to determine how many particles are available to reach defined targets [36]. In this study, the particle concentration (number of NC/ml) was evaluated using two independent methods (turbidimetry and NTA) in order to obtain an accurate result. Before estimating particle concentration by turbidimetry, it was necessary to determine particle size by photon correlation spectroscopy and the density of nanoparticles, which is calculated based on the densities of the raw materials. Taking into account that a nanoscale range requires complementary techniques in order to improve the precision of the results, data obtained using either method led to a similar particle concentration, in the same magnitude. However, the spectroscopic method (turbidimetry) is less expensive and more complex to perform, compared to NTA. Moreover, the particle concentration obtained by this method may vary by up to 10% [22]. Thus, the particle concentration obtained from NTA was chosen to calculate the doses in the subsequent *in vitro* studies. The different particle concentrations used in this study (9.85×10^{10}, 9.85×10^{11}, and 4.92×10^{12} NC/ml) correspond to 0.05, 0.57, and 2.84 mg/ml of particles, respectively.

Before starting the cytotoxicity assays, aliquots of the NC suspension were mixed with both RPMI (NC-RPMI) or MEM (NC-MEM) cell culture media to a 1:1

ratio in order to assess the behavior of the particles in these media. The physicochemical parameters evaluated (size, PDI, zeta potential) as well as the particle size distribution of nanocapsules remained in the nanometric scale, with results practically unchanged in comparison with the original NC suspension. This result may be explained considering the absence of charge of the polymer and polysorbate 80, which could prevent nanocapsules aggregation or the formation of microstructures in the presence of both cell culture media.

In order to find the particle concentration that does not harm the cells under *in vitro* conditions, cytotoxicity assays of the NC in representative cell lines of the alveolar (A549) or bronchial (Calu-3) lung regions were performed. Cellular membrane integrity and metabolic activity via mitochondrial enzymes were assessed using LDH and AB assays, respectively. As can be observed, only the particle concentration represented by the highest surface area was cytotoxic to A549 and Calu-3 cells. On the other hand, the results obtained for 9.85×10^{10} and 9.85×10^{11} NC/ml are supported by the AB test, where both A549 and Calu-3 cells remained metabolically active after 48 h of exposure to 9.85×10^{10} and 9.85×10^{11} NC/ml.

The presence of a surfactant in the NC suspension is another factor that may influence cytotoxic effects [37]. Moreover, this important structural component of nanoparticles may contribute to the internalization of such drug delivery systems into the cells, promoting drug targeting [15, 38]. Polysorbate 80 showed low cytotoxic effect in the LDH test in A549 and Calu-3 cells, regardless of its concentration. Therefore, the hypothesis of the influence of the surfactant on the cytotoxic effects shown by the higher particle concentration (4.92×10^{12} NC/ml) could be refuted. Taken together, these results show that the cytotoxic effects demonstrated only by the higher number of NC are not cell-specific. It may be suggested that this effect may be a consequence of

the physical effect of the nanoparticles due to the overexposure of these cells to a high number of particles. Based on these data, the particle concentration of 9.85 x 10^{11} NC/ml was chosen for the next experiments, since this particle concentration was not harmful to A549 and Calu-3 cells in the evaluated conditions.

The use of Calu-3 cells as a model of the airway mucosa is well established [39, 40] to study the effects and responses of several compounds as well as nanoparticles in respiratory tract. Their ability to reproduce physiological process of the airway epithelium such as transport of drugs [40], the secretion of proinflammatory cytokines [38, 41], and barrier function [14, 42] is also widely known. Moreover, this human bronchial model affords to measure TEER, which is routinely monitored and gives information about the integrity of the cell barrier. To the best of our knowledge, no previous study has specifically addressed the influence of poly(ε-caprolactone)-based polymeric nanocapsules on the epithelial barrier of Calu-3 monolayers. As previously mentioned, glucocorticoids are the therapeutics of choice for some pulmonary diseases [11, 43]. Moreover, it has been reported that glucocorticoids can increase TEER in Calu-3 [43]. So, the influence of the nanoencapsulation of DFZ on the epithelial barrier of Calu-3 cells was evaluated. For comparison, the same DFZ concentration used to prepare such NC was solubilized in a cell culture media containing DMSO at 1% (v/v) and used as non-encapsulated form of the drug (Free-DFZ). Firstly, a NC suspension containing DFZ at 0.5% (NC-DFZ) was produced. The presence of the drug did not alter the physicochemical characteristics of the original NC or particle distribution.

Regarding all TEER values, the treatments did not damage the epithelial barrier during the experiment, regardless of the presence of drug. Interestingly, measured TEER values for NC-DFZ were higher than those observed in all the other treatments after 24 h. This finding is remarkable, because the TEER measurement of the

association between NC and DFZ seems to have an additive effect on this parameter, in comparison with TEER values for unloaded NC or non-encapsulated DFZ. The injured epithelial barrier (i.e. in asthmatics and allergic rhinitis) has been reported to be an entry route for pathological agents, which in turn increase the susceptibility to allergens and viral infections [44, 45]. On the other hand, there was no significant difference between the TEER values of the NC and NC-DFZ within 48 h. Therefore, since TEER values reflect the integrity of the epithelial barrier, the association between NC and a glucocorticoid (DFZ) may be suggested as a potential approach to improve the epithelial integrity.

The permeability of compounds across the epithelial barrier depends on their integrity [42]. Therefore, a transport study to evaluate the influence of NC-DFZ on the paracellular permeability was carried out by measuring the permeability of sodium fluorescein (FluNa), a hydrophilic molecule typically used as paracellular marker. A tendency of NC-DFZ to decrease permeability was observed, corroborating the improvement of TEER values. Studies have reported that a decrease in TEER with the subsequent increase of paracellular permeability of fluorescent markers may promote the entry of viruses or allergens in the lung [46-48]. In these cases, the applicability of the NC-DFZ formulation could be proposed to minimize the lung vulnerability to pathogens due to its ability to decrease paracellular transport and to increase TEER, besides the known anti-inflammatory and immunosuppressive activities of this glucocorticoid.

In addition, inflammatory processes are frequently involved in several lung diseases (i.e. COPD, cystic fibrosis and asthma). IL-8 is one of the main cytokine released from lung epithelial cells, whose function is crucial in the recruitment of proinflammatory cells [30, 41]. The anti-inflammatory potential of NC-DFZ was

assessed by measuring IL-8 cytokine release in LPS pre-stimulated Calu-3 cells. The endotoxin LPS, derived from gram-negative bacteria, induces the release of IL-8 mainly by activation of the nuclear factor-κB (NF-κB). One of its functions is to control the transcription of inflammatory responses in immunocompetent cells [49].

Firstly, experiments without the stimulation of IL-8 by LPS (-LPS) in Calu-3 cells were carried out in order to evaluate whether NC may, by themselves, stimulate IL-8 secretion. The presence of such NC did not stimulate the release of this cytokine. In this case, the hypothesis whether this kind of nanoparticles could trigger the release of proinflammatory molecules was discarded. Moreover, the significant differences obtained for both NC-DFZ and Free-DFZ in comparison with the control after 48 h can be best explained by controlled drug release from nanocapsules.

Regarding the results obtained from the set of experiments where IL-8 secretion in Calu-3 cells was stimulated by LPS (+LPS), no significant differences between the control (cell culture media) and the drug free NC were observed, regardless of time. This result supports the idea that NC by themselves did neither induce nor reduce the secretion of IL-8 in the absence or presence of LPS, respectively. The decrease in IL-8 levels after the treatment with Free-DFZ for 24 and 48 h in comparison with the control was expected, considering the known anti-inflammatory activity of such glucocorticoid. On the other hand, the significant difference between NC-DFZ and the control (cell culture media) after 48 h strongly supports the hypothesis of controlled release of the glucocorticoid.

Then, in order to evaluate the controlled release of DFZ from the NC-DFZ formulation, an *in vitro* drug release study using dialysis bag method was performed. For comparison purposes, an ethanolic solution containing DFZ (DFZ-ES) at the same concentration as in the NC-DFZ formulation was prepared as a non-encapsulated drug

system. Regarding the release profiles obtained from both NC-DFZ and DFZ-ES, it is possible to observe the clear sustained release of the glucocorticoid from the nanoencapsulated form (NC-DFZ), reaching close to 85% of drug release only after 48 h. In contrast, the DFZ-ES formulation showed a fast diffusion profile, where more than 50% of the drug was available in the medium after 4 h. This way, the greater decrease of IL-8 promoted by the exposure of Calu-3 cells to NC-DFZ for 48 h could be explained based on the controlled release profile provided by the formulation, confirming our hypothesis. The ability to avoid the fast drug release is one of the main features of such NC [32, 50], which in turn prolongs or delays the time drugs remain active, improving therapeutic management. In this scenario, the association between NC and the glucocorticoid could be an interesting approach to restore the epithelial barrier function and to avoid the worsening of lung pathologies, with the subsequent release of the glucocorticoid to control the inflammation process. Moreover, it is important to emphasize that the prolonged effect can also be considered an important advantage, particularly for chronic pulmonary diseases, whose pharmacological management requires prolonged therapies. Under these circumstances, doses of glucocorticoids are recommended to control the inflammation, and are often administered through the oral route. However, this practice normally leads to adverse effects that could influence the clinical effect of such treatments, affecting patient compliance [11, 12].

4. Conclusion

The nanoencapsulation of the DFZ was essential to improve the integrity of the epithelial barrier as well as to decrease the paracellular permeability in Calu-3 cells. Moreover, NC-DFZ decreases IL-8 secretion, keeping anti-inflammatory efficacy based on the advantage of controlled drug release. It is possible that this effect starts after the

improvement of the epithelial barrier. Therefore, the association between these polymeric nanocapsules and a glucocorticoid is suggested as a potential and innovative therapeutic approach for pulmonary diseases, since it combines the ability to restore the epithelial barrier integrity and anti-inflammatory effects.

Declaration of interest:

The authors report no conflicts of interest. The authors alone are responsible for the content and writing of the article.

Acknowledgements:

Rigo, LA is grateful to CAPES/DAAD/CNPQ for his PhD scholarship. The authors are also thankful for the financial support from CNPq, CAPES, and FAPERGS.

References:

[1] A.F. Ourique, A. Melero, C.d.B.d. Silva, U.F. Schaefer, A.R. Pohlmann, S.S. Guterres, C.-M. Lehr, K.-H. Kostka, R.C.R. Beck, Improved photostability and reduced skin permeation of tretinoin: Development of a semisolid nanomedicine, European Journal of Pharmaceutics and Biopharmaceutics, 79 (2011) 95-101.

[2] M.C. Fontana, J.F. Rezer, K. Coradini, D.B. Leal, R.C. Beck, Improved efficacy in the treatment of contact dermatitis in rats by a dermatological nanomedicine containing clobetasol propionate, European journal of pharmaceutics and biopharmaceutics: official journal of Arbeitsgemeinschaft fur Pharmazeutische Verfahrenstechnik e.V, 79 (2011) 241-249.

[3] E. Schultze, A. Ourique, V.C. Yurgel, K.R. Begnini, H. Thurow, P.M.M. de Leon, V.F. Campos, O.A. Dellagostin, S.R. Guterres, A.R. Pohlmann, F.K. Seixas, R.C.R. Beck, T. Collares, Encapsulation in lipid-core nanocapsules overcomes lung cancer cell resistance to tretinoin, European Journal of Pharmaceutics and Biopharmaceutics, 87 (2014) 55-63.

[4] K. Coradini, F.O. Lima, C.M. Oliveira, P.S. Chaves, M.L. Athayde, L.M. Carvalho, R.C.R. Beck, Co-encapsulation of resveratrol and curcumin in lipid-core nanocapsules improves their in vitro antioxidant effects, European Journal of Pharmaceutics and Biopharmaceutics, 88 (2014) 178-185.

[5] M.L. Marchiori, G. Lubini, G. Dalla Nora, R.B. Friedrich, M.C. Fontana, A.F. Ourique, M.O. Bastos, L.A. Rigo, C.B. Silva, S.B. Tedesco, R.C. Beck, Hydrogel containing dexamethasone-loaded nanocapsules for cutaneous administration: preparation, characterization, and in vitro drug release study, Drug development and industrial pharmacy, 36 (2010) 962-971.

[6] V.C. Mosqueira, P. Legrand, G. Barratt, Surface-modified and conventional nanocapsules as novel formulations for parenteral delivery of halofantrine, Journal of nanoscience and nanotechnology, 6 (2006) 3193-3202.

[7] A.F. Ourique, S. Azoubel, C.V. Ferreira, C.B. Silva, M.C. Marchiori, A.R. Pohlmann, S.S. Guterres, R.C. Beck, Lipid-core nanocapsules as a nanomedicine for parenteral administration of tretinoin: development and in vitro antitumor activity on human myeloid leukaemia cells, Journal of biomedical nanotechnology, 6 (2010) 214-223.

[8] U. Pison, T. Welte, M. Giersig, D.A. Groneberg, Nanomedicine for respiratory diseases, European journal of pharmacology, 533 (2006) 341-350.

[9] J.C. Sung, B.L. Pulliam, D.A. Edwards, Nanoparticles for drug delivery to the lungs, Trends in biotechnology, 25 (2007) 563-570.

[10] S. Azarmi, W.H. Roa, R. Löbenberg, Targeted delivery of nanoparticles for the treatment of lung diseases, Advanced Drug Delivery Reviews, 60 (2008) 863-875.

[11] R. Newton, R. Leigh, M.A. Giembycz, Pharmacological strategies for improving the efficacy and therapeutic ratio of glucocorticoids in inflammatory lung diseases, Pharmacol Ther, 125 (2010) 286-327.

[12] C. Boardman, L. Chachi, A. Gavrila, C.R. Keenan, M.M. Perry, Y.C. Xia, H. Meurs, P. Sharma, Mechanisms of glucocorticoid action and insensitivity in airways disease, Pulmonary Pharmacology & Therapeutics, 29 (2014) 129-143.

[13] M. Hittinger, J. Juntke, S. Kletting, N. Schneider-Daum, C. de Souza Carvalho, C.-M. Lehr, Preclinical safety and efficacy models for pulmonary drug delivery of antimicrobials with focus on in vitro models, Advanced Drug Delivery Reviews, 85 (2015) 44-56.

[14] B. Forbes, C. Ehrhardt, Human respiratory epithelial cell culture for drug delivery applications, European Journal of Pharmaceutics and Biopharmaceutics, 60 (2005) 193-205.

[15] N. Grabowski, H. Hillaireau, J. Vergnaud, L.A. Santiago, S. Kerdine-Romer, M. Pallardy, N. Tsapis, E. Fattal, Toxicity of surface-modified PLGA nanoparticles toward lung alveolar epithelial cells, International journal of pharmaceutics, 454 (2013) 686-694.

[16] N. Nafee, M. Schneider, U.F. Schaefer, C.-M. Lehr, Relevance of the colloidal stability of chitosan/PLGA nanoparticles on their cytotoxicity profile, International journal of pharmaceutics, 381 (2009) 130-139.

[17] A. Beyerle, O. Merkel, T. Stoeger, T. Kissel, PEGylation affects cytotoxicity and cell-compatibility of poly(ethylene imine) for lung application: Structure–function relationships, Toxicology and applied pharmacology, 242 (2010) 146-154.

[18] J.R. Ferraris, T. Pasqualini, G. Alonso, S. Legal, P. Sorroche, A.M. Galich, H. Jasper, Effects of deflazacort vs. methylprednisone: a randomized study in kidney transplant patients, Pediatric nephrology (Berlin, Germany), 22 (2007) 734-741.

[19] M.C. Fontana, K. Coradini, S.S. Guterres, A.R. Pohlmann, R.C. Beck, Nanoencapsulation as a way to control the release and to increase the photostability of clobetasol propionate: influence of the nanostructured system, Journal of biomedical nanotechnology, 5 (2009) 254-263.

[20] M.C. Fontana, K. Coradini, A.R. Pohlmann, S.S. Guterres, R.C. Beck, Nanocapsules prepared from amorphous polyesters: effect on the physicochemical characteristics, drug release, and photostability, Journal of nanoscience and nanotechnology, 10 (2010) 3091-3099.

[21] A. Scremin, M. Piazzon, M.A.S. Silva, G. Kuminek, G.M. Correa, N. Paulino, S.G. Cardoso, Spectrophotometric and HPLC determination of deflazacort in pharmaceutical dosage forms, Brazilian Journal of Pharmaceutical Sciences, 46 (2010) 281-287.

[22] F.S. Poletto, E. Jäger, L. Cruz, A.R. Pohlmann, S.S. Guterres, The effect of polymeric wall on the permeability of drug-loaded nanocapsules, Materials Science and Engineering: C, 28 (2008) 472-478.

[23] F.S. Poletto, L.A. Fiel, M.V. Lopes, G. Schaab, A.M.O. Gomes, S.S. Guterres, B. Rossi-Bergmann, A.R. Pohlmann, Fluorescent-Labeled Poly(e-caprolactone) Lipid-Core Nanocapsules: Synthesis, Physicochemical Properties and Macrophage Uptake, Journal of Colloid Science and Biotechnology, 1 (2012) 89-98.

[24] V. Filipe, A. Hawe, W. Jiskoot, Critical Evaluation of Nanoparticle Tracking Analysis (NTA) by NanoSight for the Measurement of Nanoparticles and Protein Aggregates, Pharm Res, 27 (2010) 796-810.

[25] J.A. Gallego-Urrea, J. Tuoriniemi, M. Hassellöv, Applications of particle-tracking analysis to the determination of size distributions and concentrations of nanoparticles in environmental, biological and food samples, TrAC Trends in Analytical Chemistry, 30 (2011) 473-483.

[26] E. Jager, C.G. Venturini, F.S. Poletto, L.M. Colome, J.P. Pohlmann, A. Bernardi, A.M. Battastini, S.S. Guterres, A.R. Pohlmann, Sustained release from lipid-core nanocapsules by varying the core viscosity and the particle surface area, Journal of biomedical nanotechnology, 5 (2009) 130-140.

[27] R. Hamid, Y. Rotshteyn, L. Rabadi, R. Parikh, P. Bullock, Comparison of alamar blue and MTT assays for high through-put screening, Toxicology in vitro: an international journal published in association with BIBRA, 18 (2004) 703-710.

[28] F. Bonnier, M.E. Keating, T.P. Wróbel, K. Majzner, M. Baranska, A. Garcia-Munoz, A. Blanco, H.J. Byrne, Cell viability assessment using the Alamar blue assay: A comparison of 2D and 3D cell culture models, Toxicology in Vitro, 29 (2015) 124-131.

[29] K. Elbert, U. Schäfer, H.-J. Schäfers, K.-J. Kim, V.L. Lee, C.-M. Lehr, Monolayers of Human Alveolar Epithelial Cells in Primary Culture for Pulmonary Absorption and Transport Studies, Pharm Res, 16 (1999) 601-608.

[30] S.L. Kunkel, T. Standiford, K. Kasahara, R.M. Strieter, Interleukin-8 (IL-8): the major neutrophil chemotactic factor in the lung, Experimental lung research, 17 (1991) 17-23.

[31] R.J. Carmody, Y.H. Chen, Nuclear factor-kappaB: activation and regulation during toll-like receptor signaling, Cellular & molecular immunology, 4 (2007) 31-41.

[32] K.S. Soppimath, T.M. Aminabhavi, A.R. Kulkarni, W.E. Rudzinski, Biodegradable polymeric nanoparticles as drug delivery devices, Journal of Controlled Release, 70 (2001) 1-20.

[33] J.S. Almeida, F. Lima, S.D. Ros, L.O. Bulhoes, L.M. de Carvalho, R.C. Beck, Nanostructured Systems Containing Rutin: In Vitro Antioxidant Activity and Photostability Studies, Nanoscale research letters, 5 (2010) 1603-1610.

[34] A.F. Ourique, A.R. Pohlmann, S.S. Guterres, R.C. Beck, Tretinoin-loaded nanocapsules: Preparation, physicochemical characterization, and photostability study, International journal of pharmaceutics, 352 (2008) 1-4.

[35] A. Jager, V. Stefani, S.S. Guterres, A.R. Pohlmann, Physico-chemical characterization of nanocapsule polymeric wall using fluorescent benzazole probes, International journal of pharmaceutics, 338 (2007) 297-305.

[36] A. Elsaesser, C.V. Howard, Toxicology of nanoparticles, Advanced Drug Delivery Reviews, 64 (2012) 129-137.

[37] N. Schöler, C. Olbrich, K. Tabatt, R.H. Müller, H. Hahn, O. Liesenfeld, Surfactant, but not the size of solid lipid nanoparticles (SLN) influences viability and cytokine production of macrophages, International journal of pharmaceutics, 221 (2001) 57-67.

[38] S. Mura, H. Hillaireau, J. Nicolas, B. Le Droumaguet, C. Gueutin, S. Zanna, N. Tsapis, E. Fattal, Influence of surface charge on the potential toxicity of PLGA nanoparticles towards Calu-3 cells, International journal of nanomedicine, 6 (2011) 2591-2605.

[39] K.A. Foster, M.L. Avery, M. Yazdanian, K.L. Audus, Characterization of the Calu-3 cell line as a tool to screen pulmonary drug delivery, International journal of pharmaceutics, 208 (2000) 1-11.

[40] B.I. Florea, M.L. Cassara, H.E. Junginger, G. Borchard, Drug transport and metabolism characteristics of the human airway epithelial cell line Calu-3, Journal of controlled release: official journal of the Controlled Release Society, 87 (2003) 131-138.

[41] E. Alfaro-Moreno, V. Torres, J. Miranda, L. Martínez, C. García-Cuellar, T.S. Nawrot, B. Vanaudenaerde, P. Hoet, P. Ramírez-López, I. Rosas, B. Nemery, A.R. Osornio-Vargas, Induction of IL-6 and inhibition of IL-8 secretion in the human airway cell line Calu-3 by urban particulate matter collected with a modified method of PM sampling, Environmental Research, 109 (2009) 528-535.

[42] I.I. Forbes, Human airway epithelial cell lines for in vitro drug transport and metabolism studies, Pharmaceutical science & technology today, 3 (2000) 18-27.

[43] A. Sekiyama, Y. Gon, M. Terakado, I. Takeshita, Y. Kozu, S. Maruoka, K. Matsumoto, S. Hashimoto, Glucocorticoids enhance airway epithelial barrier integrity, International immunopharmacology, 12 (2012) 350-357.

[44] Y. Wang, C. Bai, K. Li, K.B. Adler, X. Wang, Role of airway epithelial cells in development of asthma and allergic rhinitis, Respiratory Medicine, 102 (2008) 949-955.

[45] S.T. Holgate, D.E. Davies, S. Puddicombe, A. Richter, P. Lackie, J. Lordan, P. Howarth, Mechanisms of airway epithelial damage: epithelial-mesenchymal interactions in the pathogenesis of asthma, European Respiratory Journal, 22 (2003) 24s-29s.

[46] F. Rezaee, N. Meednu, J.A. Emo, B. Saatian, T.J. Chapman, N.G. Naydenov, A. De Benedetto, L.A. Beck, A.I. Ivanov, S.N. Georas, Polyinosinic:polycytidylic acid induces protein kinase D-dependent disassembly of apical junctions and barrier dysfunction in airway epithelial cells, The Journal of allergy and clinical immunology, 128 (2011) 1216-1224 e1211.

[47] S. Runswick, T. Mitchell, P. Davies, C. Robinson, D.R. Garrod, Pollen proteolytic enzymes degrade tight junctions, Respirology (Carlton, Vic.), 12 (2007) 834-842.

[48] R. Vinhas, L. Cortes, I. Cardoso, V.M. Mendes, B. Manadas, A. Todo-Bom, E. Pires, P. Verissimo, Pollen proteases compromise the airway epithelial barrier through degradation of transmembrane adhesion proteins and lung bioactive peptides, Allergy, 66 (2011) 1088-1098.

[49] W. Abate, A.A. Alghaithy, J. Parton, K.P. Jones, S.K. Jackson, Surfactant lipids regulate LPS-induced interleukin-8 production in A549 lung epithelial cells by inhibiting translocation of TLR4 into lipid raft domains, Journal of lipid research, 51 (2010) 334-344.

[50] A. Kumari, S.K. Yadav, S.C. Yadav, Biodegradable polymeric nanoparticles based drug delivery systems, Colloids and Surfaces B: Biointerfaces, 75 (2010) 1-18.

Figure captions

Figure 1: Sizes distribution profiles obtained by laser diffraction considering the volume for polymeric nanocapsules (NC), polymeric nanocapsules and MEM (NC-MEM), polymeric nanocapsules and RPMI (NC-RPMI), and polymeric nanocapsules containing deflazacort (NC-DFZ) (*n = 3*).

Figure 2: Cell viability of the (A) A549 and (B) Calu-3 cell lines exposed to polymeric nanocapsules at different particle concentrations after 2, 24, and 48 h (*n = 3*) obtained using the lactate dehydrogenase (LDH) method.

Figure 3: Cell viability of the (A) A549 and (B) Calu-3 cell lines exposed to polymeric nanocapsules at different particle concentrations after 2, 24, and 48 h (*n = 3*) obtained using the Alamar Blue (AB) method.

Figure 4: Cell viability of the (A) A549 and (B) Calu-3 cell lines exposed to polymeric nanocapsules at different particle concentrations after 2, 24, and 48 h (*n = 3*) obtained using the lactate dehydrogenase (LDH) method.

Figure 5: Cell viability of the (A) A549 and (B) Calu-3 cell lines exposed to polysorbate 80 at different concentrations after 2, 24, and 48 h (*n = 3*) obtained using the Alamar blue (AB) method.

Figure 6: Transepithelial electrical resistance (TEER) measurements of the Calu-3 cells after exposure to polymeric nanocapsules (NC), polymeric nanocapsules containing deflazacort (NC-DFZ), and non-encapsulated form of deflazacort (Free-DFZ). Cell culture medium (CCM) was used as control (*n = 3*).

Figure 7: Apparent permeability coefficients (P_{app}) of sodium fluorescein after 24 h of exposure to polymeric nanocapsules (NC), polymeric nanocapsules containing deflazacort (NC-DFZ), and non-encapsulated form of deflazacort (Free-DFZ) in Calu-3 cell lines. Cell culture medium (CCM) was used as control (*n = 3*).

Figure 8: Levels of IL-8 cytokine in (A) non-stimulated (-LPS) or (B) stimulated LPS (+LPS) after 24 and 48 h of exposure to polymeric nanocapsules (NC), polymeric nanocapsules containing deflazacort (NC-DFZ), and non-encapsulated form of

deflazacort (DFZ) in Calu-3 cells. Cell culture medium (CCM) was used as control (*n = 3*).

Figure 9: *In vitro* drug release/diffusion profiles of non-encapsulated deflazacort in an ethanolic solution (DFZ-ES) and from polymeric nanocapsules (NC-DFZ) (*n = 3*).

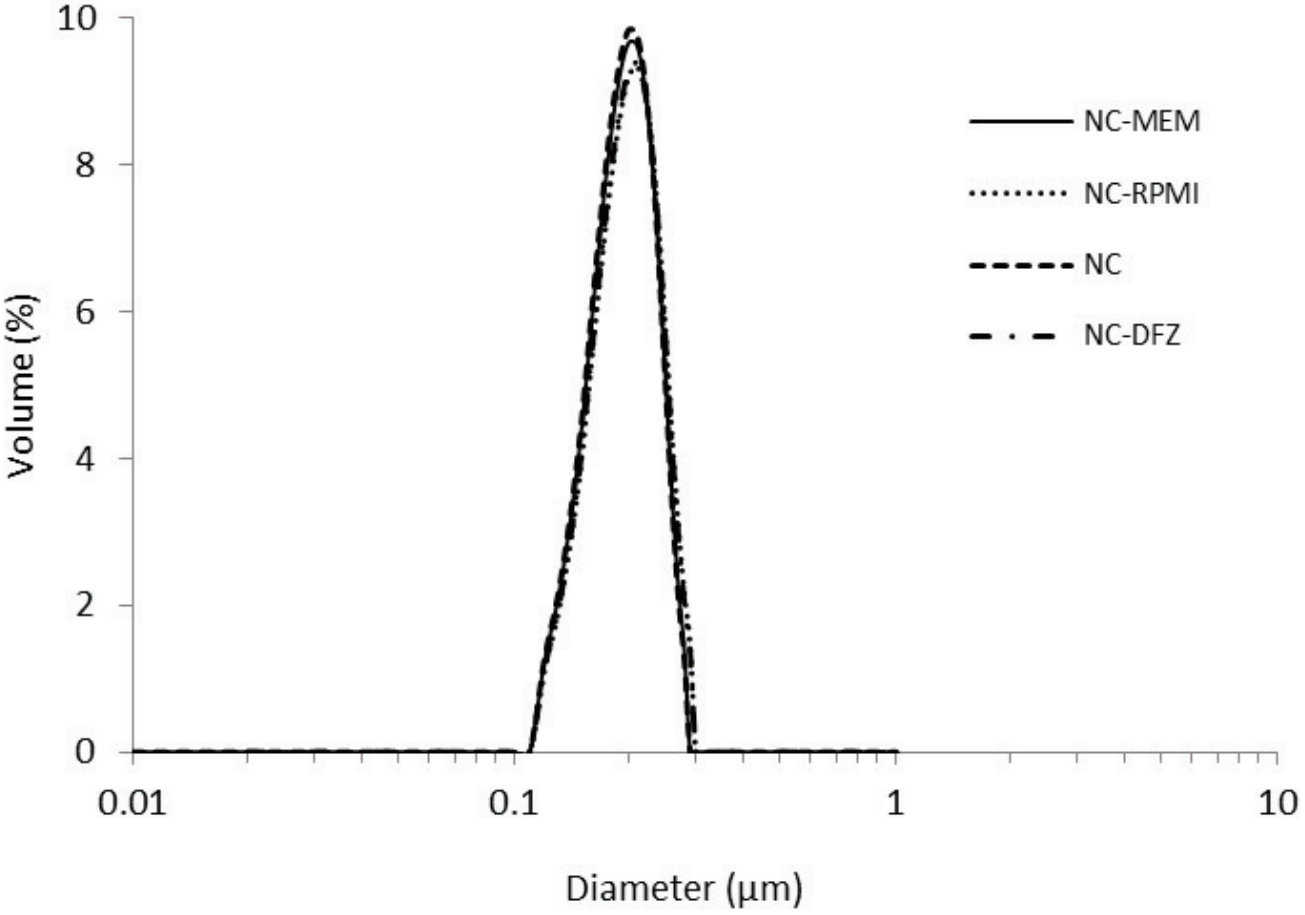
10
8
6
4
2
0
Volume (%)
0.01
0.1
1
10
Diameter (µm)
NC-MEM
NC-RPMI
NC
NC-DFZ

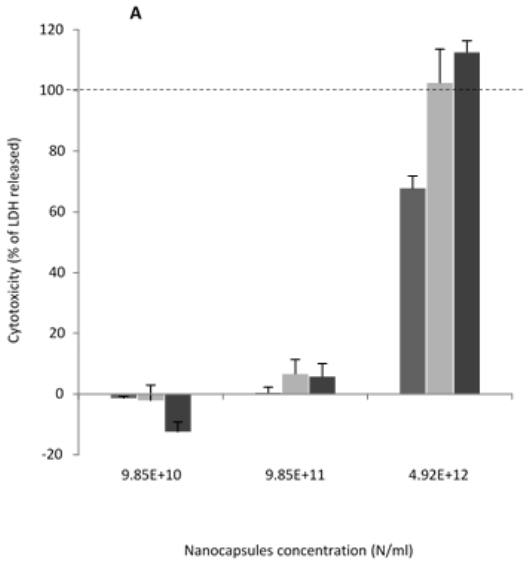
A
120
100
80
60
40
20
0
-20
Cytotoxicity (% of LDH released)
9.85E+10
9.85E+11
4.92E+12
Nanocapsules concentration (N/ml)

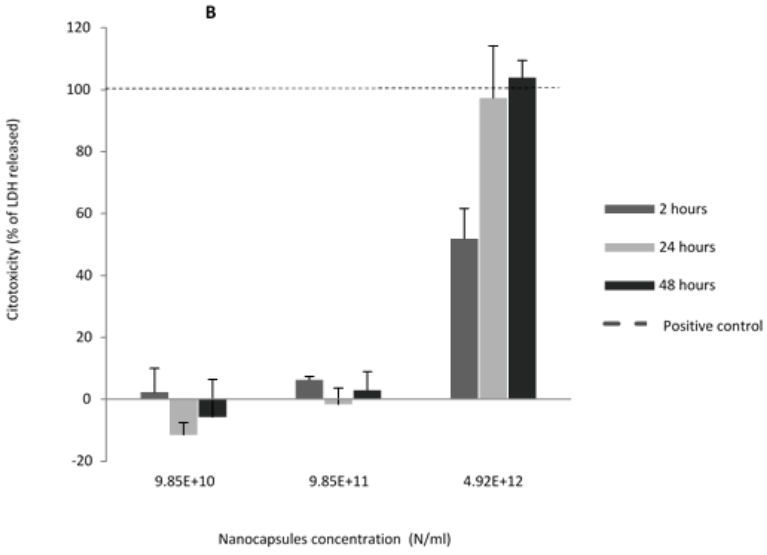
B
120
100
80
60
40
20
0
-20
Citotoxicity (% of LDH released)
9.85E+10
9.85E+11
4.92E+12
Nanocapsules concentration (N/ml)
2 hours
24 hours
48 hours
Positive control

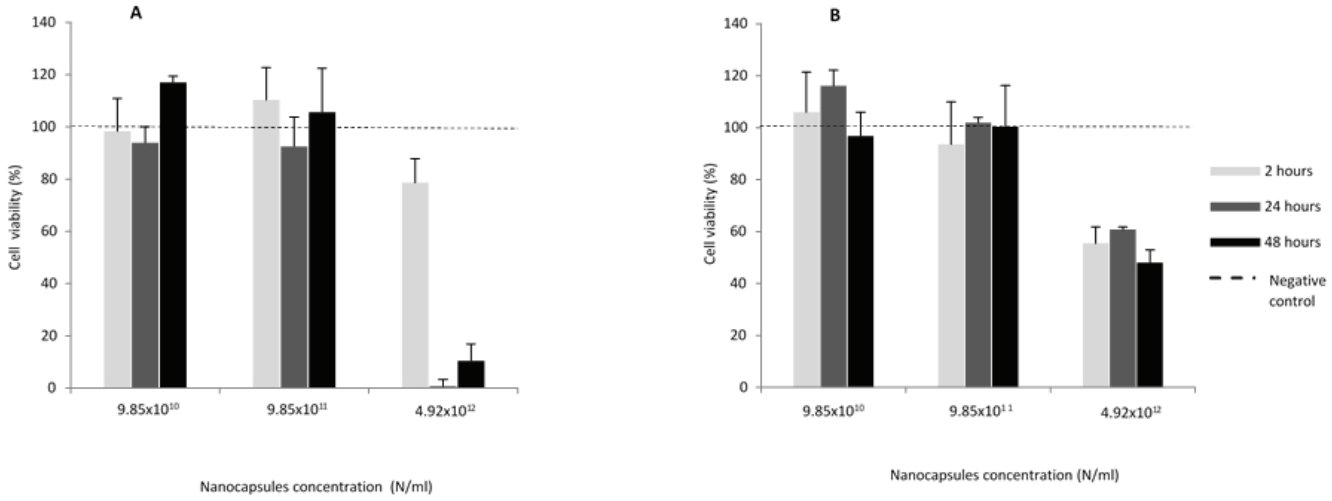
A
B
140
120
100
80
60
40
20
0
Cell viability (%)
9.85x10^10
9.85x10^11
4.92x10^12
Nanocapsules concentration (N/ml)
2 hours
24 hours
48 hours
Negative control

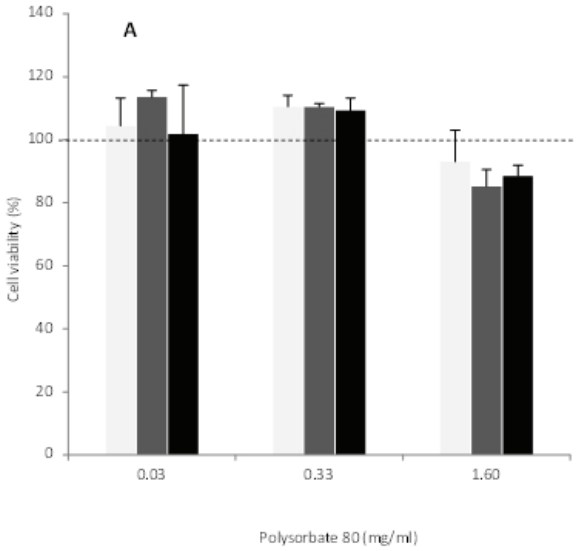
A
140
120
100
80
60
40
20
0
Cell viability (%)
0.03
0.33
1.60
Polysorbate 80 (mg/ml)

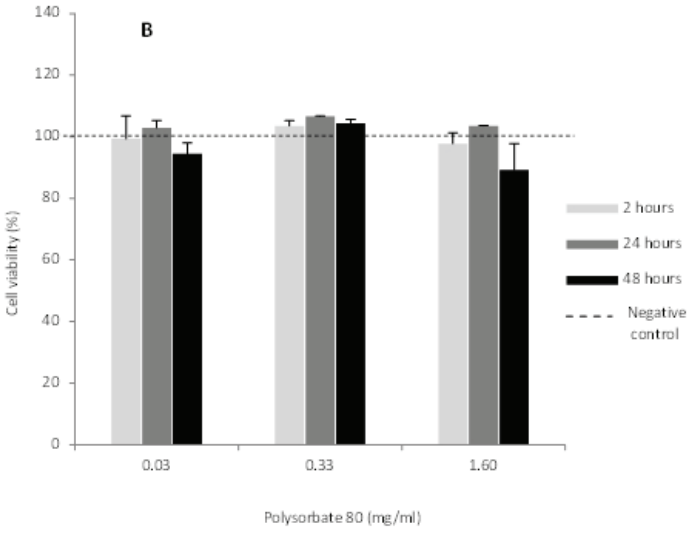
B
140
120
100
80
60
40
20
0
Cell viability (%)
0.03
0.33
1.60
Polysorbate 80 (mg/ml)
2 hours
24 hours
48 hours
Negative control

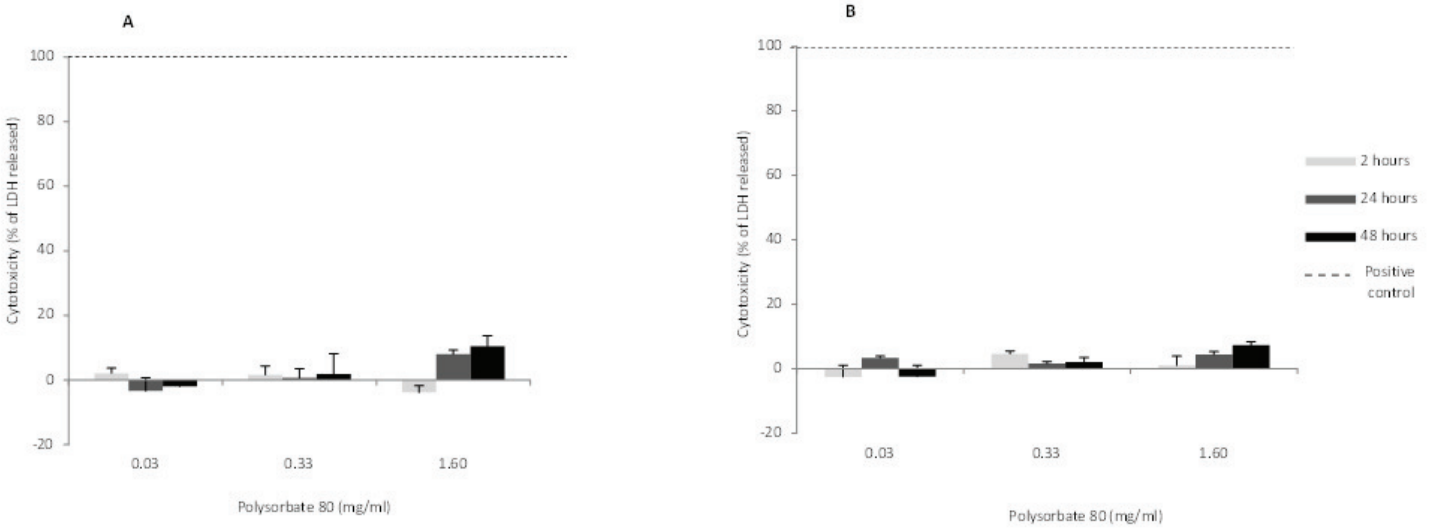
A
B
100
80
60
40
20
0
-20
Cytotoxicity (% of LDH released)
0.03
0.33
1.60
Polysorbate 80 (mg/ml)
2 hours
24 hours
48 hours
Positive control

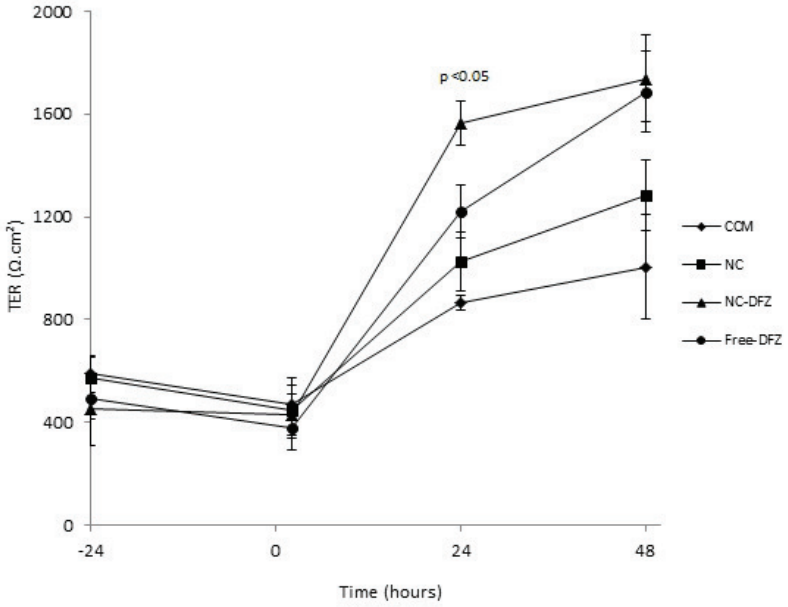
2000
1600
1200
800
400
0
TER (Ω.cm²)
p <0.05
-24
0
24
48
Time (hours)
CCM
NC
NC-DFZ
Free-DFZ

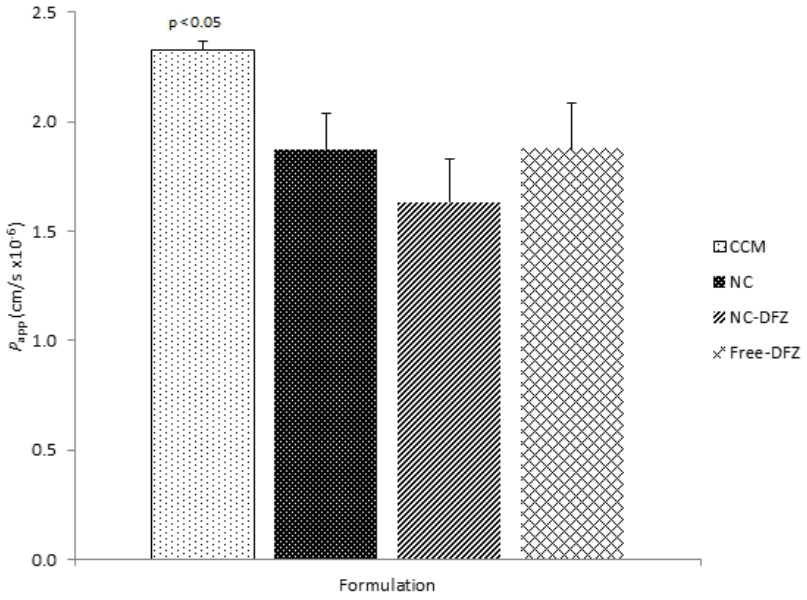
p < 0.05
2.5
2.0
1.5
1.0
0.5
0.0
P_{app} (cm/s x10^{-6})
Formulation
CCM
NC
NC-DFZ
Free-DFZ

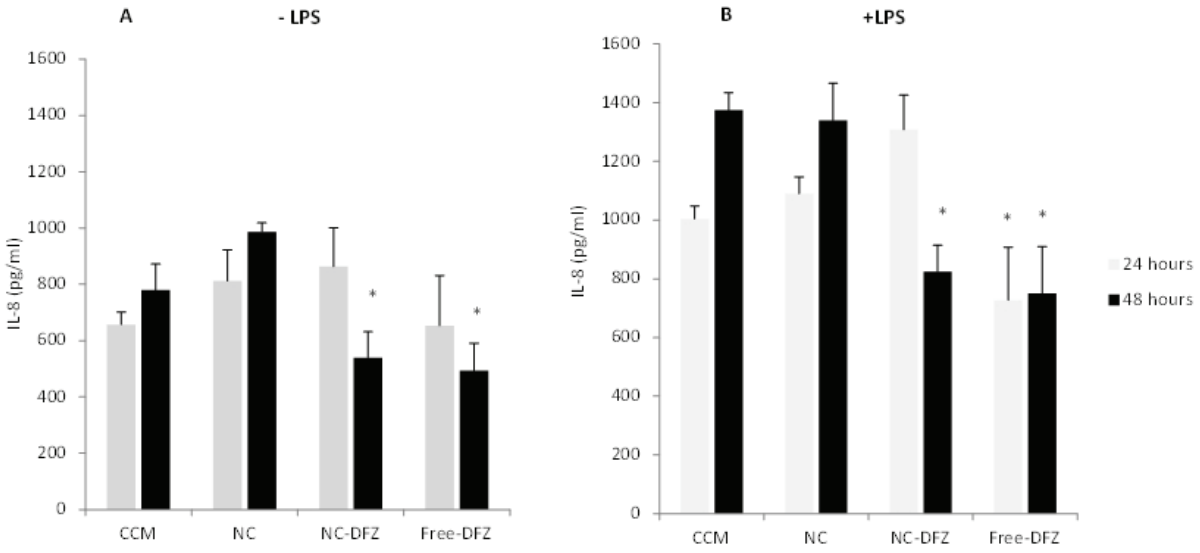
A
- LPS
IL-8 (pg/ml)
1600
1400
1200
1000
800
600
400
200
0
CCM
NC
NC-DFZ
Free-DFZ
*
*
B
+LPS
IL-8 (pg/ml)
1600
1400
1200
1000
800
600
400
200
0
CCM
NC
NC-DFZ
Free-DFZ
*
*
*
24 hours
48 hours

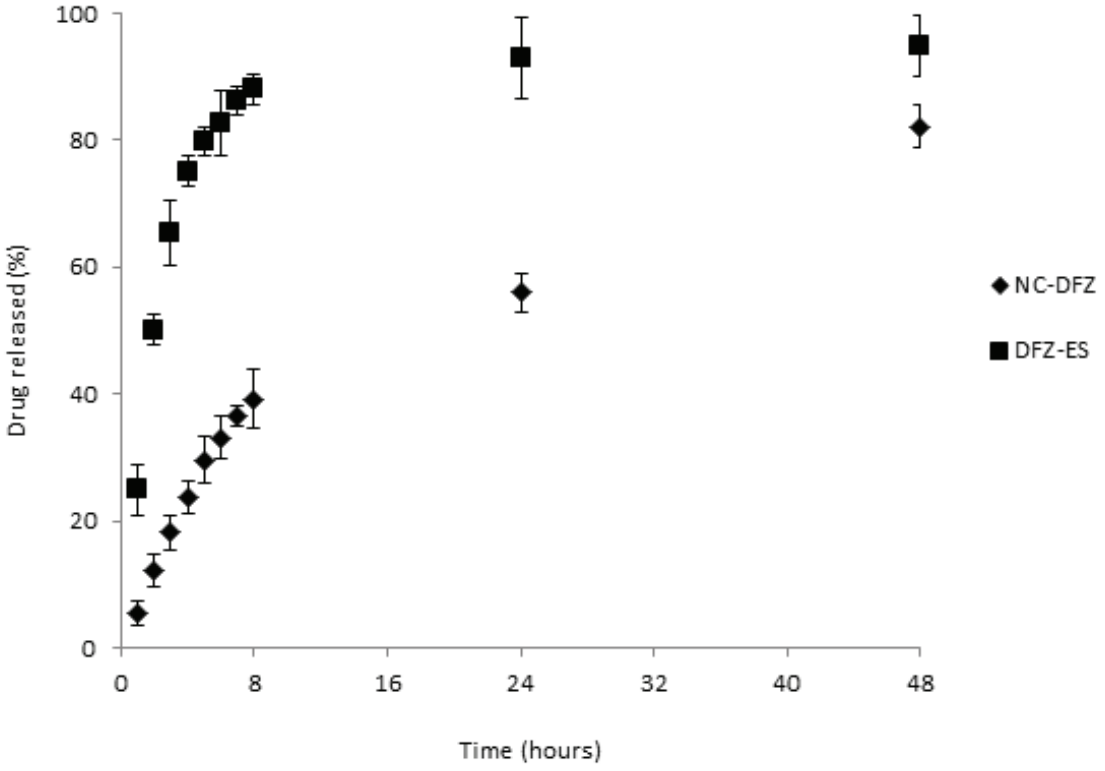
100
80
60
40
20
0
Drug released (%)
0
8
16
24
32
40
48
Time (hours)
NC-DFZ
DFZ-ES

Table 1: Particle size distribution of polymeric nanocapsules.

Formulation	Particle size distribution			
	$d_{0.1}$ (μm)	$d_{0.5}$ (μm)	$d_{0.9}$ (μm)	SPAN
NC	0.067	0.133	0.265	1.486
NC-DFZ	0.069	0.142	0.297	1.610
NC-MEM	0.066	0.132	0.268	1.529
NC-RPMI	0.068	0.136	0.277	1.541

NC, polymeric nanocapsules; NC-DFZ, polymeric nanocapsules containing deflazacort; NC-MEM, polymeric nanocapsules mixed with MEM cell culture medium; NC-RPMI, polymeric nanocapsules mixed with RPMI cell culture medium.

Table 2. Physicochemical characteristics of polymeric nanocapsules obtained by photon correlation spectroscopy.

Formulation	Particle size (nm)	PDI	Zeta potential (mV)
NC	200 ± 10	0.08 ± 0.04	-8.01 ± 0.65
NC-DFZ	202 ± 8	0.09 ± 0.02	-7.58 ± 0.89
NC-RPMI	193 ± 7	0.07 ± 0.02	-7.34 ± 1.13
NC-MEM	202 ± 3	0.09 ± 0.04	-7.50 ± 0.72

PDI, polydispersity index; NC, polymeric nanocapsules; NC-DFZ, polymeric nanocapsules containing deflazacort; NC-MEM, polymeric nanocapsules mixed with MEM cell culture medium; NC-RPMI, polymeric nanocapsules mixed with RPMI cell culture medium.